

Research Article

Nonfragile H_∞ Stabilizing Nonlinear Systems Described by Multivariable Hammerstein Models

Zeineb Rayouf, Chekib Ghorbel , and Naceur Benhadj Braiek 

Laboratory of Advanced Systems, Polytechnic High School of Tunisia, University of Carthage, BP 743, 2078, La Marsa, Tunisia

Correspondence should be addressed to Chekib Ghorbel; chekib.ghorbel@enit.rnu.tn

Received 17 September 2020; Revised 15 November 2020; Accepted 2 February 2021; Published 19 February 2021

Academic Editor: Alina Gavrilu

Copyright © 2021 Zeineb Rayouf et al. This is an open access article distributed under the Creative Commons Attribution License, which permits unrestricted use, distribution, and reproduction in any medium, provided the original work is properly cited.

This paper presents the problem of robust and nonfragile stabilization of nonlinear systems described by multivariable Hammerstein models. The objective is focused on the design of a nonfragile feedback controller such that the resulting closed-loop system is globally asymptotically stable with robust H_∞ disturbance attenuation in spite of controller gain variations. First, the parameters of linear and nonlinear blocks characterizing the multivariable Hammerstein model structure are separately estimated by using a subspace identification algorithm. Second, approximate inverse nonlinear functions of polynomial form are proposed to deal with nonbijective invertible nonlinearities. Thereafter, the Takagi–Sugeno model representation is used to decompose the composition of the static nonlinearities and their approximate inverses in series with the linear subspace dynamic submodel into linear fuzzy parts. Besides, sufficient stability conditions for the robust and nonfragile controller synthesis based on quadratic Lyapunov function, H_∞ criterion, and linear matrix inequality approach are provided. Finally, a numerical example based on twin rotor multi-input multi-output system is considered to demonstrate the effectiveness.

1. Introduction

The nonlinear modeling of real-world processes, which are complex in nature, remains a challenging problem. However, much research works remain to be done for realization on nonlinear mathematical models that accurately represent these processes [1–4]. One way to cope with this difficulty is to use the block-oriented nonlinear models [5–7], which represent a combination of static nonlinear components and linear dynamic submodels. These models are popular in nonlinear modeling because of their advantages to be quite simple to understand and easy to use [8], for instance, the Hammerstein model (a static nonlinear component followed by a linear submodel), Wiener model (a linear submodel followed by a static nonlinear component), and Hammerstein–Wiener model (a linear submodel sandwiched by two static nonlinearities or vice versa). In particular, the simplest model structure of them is the Hammerstein model, which has been extensively used for modeling electrical generators [9], chemical processes [10], and biological processes [11] and is also used in signal processing applications [12].

Over the past decades, various parametric subspace identification methods have been very successful for the modeling of multivariable Hammerstein models. These methods include the iterative identification approach [13, 14], the overparameterization method [15], the blind approach [16], the instrumental variables method [17], the stochastic approach [18], and the least square support vector machines [19]. Most of them are based on the numerical subspace state-space system identification algorithm [20], the canonical variate analysis approach [21], and the multivariable output error state-space (MOESP) algorithm [10, 22].

From a control point of view, the conventional control scheme of a Hammerstein model has introduced the inverse of the nonlinear block into the appropriate place. This leads to reject the nonlinearity effect in the controller design [23]. Hence, the nonlinear control strategy problem is converted into a new linear one; also, any standard linear controller for a linear dynamic submodel can be applied. It should be a strong assumption that this nonlinearity is supposed to be exactly invertible [24–26]. In contrast, the performance of

this strategy becomes limited when the nonlinear component function is not bijective. In this view, many algorithms and approximations are used in the literature to determine the corresponding nonlinearity inverse. One may refer to latest research works based on polynomial form approximation [23, 27, 28], Bernstein–Bezier neural network [29], De Boor algorithm [30], and rational B-spline model approximation [31].

On the other hand, many studies have been devoted to the robust and nonfragile controller design problem for complex systems. Indeed, it is clear that relatively small perturbations in controller gain parameters can result in instability of the controlled system [32, 33]. Hence, it is necessary that any controller should be able to tolerate some bounded uncertainty in its parameters [3, 34, 35]. For instance, a nonfragile controller for uncertain nonlinear networked control systems was proposed in [36]. In [37], a nonfragile robust controller was investigated for uncertain large-scale systems. Lee et al. [38] proposed a nonfragile fuzzy H_∞ controller for nonlinear systems described in Takagi–Sugeno (T-S) fuzzy model, and so on. To our best knowledge, the nonfragile control problem for Hammerstein models has not been treated yet.

In this framework, we use the MOESP subspace identification algorithm, which mainly involves two aspects: (i) determining the order of the system and obtaining the structure of the estimated state-space model and (ii) identifying the mathematical model's unknown parameters from the available input-output data [10]. Afterwards, we propose a new control strategy for multivariable Hammerstein model including approximate inverse nonlinearities of polynomial form. Using then the T-S fuzzy model representation [1, 2, 34, 39], the composed nonlinear functions of the considered static nonlinearities and their approximate inverses in series with the linear dynamic submodel are decomposed into linear fuzzy parts. The resulting model is finally obtained by interpolating the constructed linear fuzzy parts through nonlinear fuzzy membership functions [2, 4, 35, 40]. In this regard, a nonfragile H_∞ feedback controller is designed subject to controller gain variations guaranteeing both the stability and disturbance attenuation of the controlled nonlinear system.

The main contributions of this paper are listed as follows:

- (i) A modified subspace-based algorithm is used to identify nonlinear systems described by multivariable Hammerstein models.
- (ii) Compared with the existing results using the normal nonlinearity inversion method, we derive a new control strategy based on approximate inverse nonlinear functions of polynomial form. Furthermore, we appeal the T-S fuzzy model representation to decompose the existing nonlinearities and facilitate the controller synthesis.
- (iii) From a control point of view, we develop a robust and nonfragile H_∞ controller with variation in the control law that guarantees both the asymptotic

stability and disturbance attenuation of the controlled nonlinear system and its identified multivariable Hammerstein model.

- (iv) Besides, sufficient controller design conditions in terms of linear matrix inequalities (LMIs) are established, which can be efficiently solved by convex optimization techniques.

Following the introduction, this paper is organized as follows. The subspace identification method for multivariable Hammerstein model is presented in Section 2. Section 3 is reserved to the stability analysis and nonfragile H_∞ control synthesis. A numerical example based on twin rotor multi-input multi-output system (TRMS) is considered in Section 4 to demonstrate the effectiveness.

2. MOESP Algorithm-Based Subspace Identification

We consider the multi-input multi-output (MIMO) Hammerstein model configuration, as depicted in Figure 1. As mentioned obviously, the model's structure consists of m -static nonlinearities $f_i(\cdot)$ followed by a linear dynamic submodel.

More precisely, each nonlinear component $f_i(\cdot)$, for $i = 1, 2, \dots, m$, is characterized by the following form:

$$v_{i,k} = f_i(u_{i,k}) = \lambda_{i1}u_{i,k} + \lambda_{i2}u_{i,k}^2 + \dots + \lambda_{iv}u_{i,k}^v, \quad (1)$$

and the linear dynamic submodel is described by the following state-space representation:

$$\begin{cases} x_{k+1} = Ax_k + B_1V_k + B_2w_k, \\ Y_k = Cx_k + DV_k + \varepsilon_k, \end{cases} \quad (2)$$

where $x_k \in \mathbb{R}^n$ is the state vector, $V_k = (v_{1,k} \ v_{2,k} \ \dots \ v_{m,k})^\perp$ is the unmeasurable output, $w_k \in \mathbb{R}^n$ is the external disturbance vector, $\varepsilon_k \in \mathbb{R}^q$ is the measurement noise vector, $u_k = (u_{1,k} \ u_{2,k} \ \dots \ u_{m,k})^\perp$ is the input vector, $Y_k = (y_{1,k} \ y_{2,k} \ \dots \ y_{q,k})^\perp$ is the output vector, and the notation (\perp) denotes the transposed element. $A \in \mathbb{R}^{n \times n}$, $B_1 = (B_{11} \ B_{12} \ \dots \ B_{1m}) \in \mathbb{R}^{n \times m}$, $B_2 \in \mathbb{R}^{n \times n}$, $C \in \mathbb{R}^{q \times n}$, and $D = (D_1 \ D_2 \ \dots \ D_m) \in \mathbb{R}^{q \times m}$ are unknown state-space matrices.

By substituting (1) into (2), we obtain the following open-loop model:

$$\begin{cases} x_{k+1} = Ax_k + B_1^\lambda U_k + B_2w_k, \\ Y_k = Cx_k + D^\lambda U_k + \varepsilon_k, \end{cases} \quad (3)$$

where $U_k = (U_{1,k} \ U_{2,k} \ \dots \ U_{m,k})^\perp$, $U_{i,k} = (u_{i,k} \ u_{i,k}^2 \ \dots \ u_{i,k}^v)^\perp$, $B_1^\lambda = (B_{11}^\lambda \ B_{12}^\lambda \ \dots \ B_{1m}^\lambda)$, $D^\lambda = (D_1^\lambda \ D_2^\lambda \ \dots \ D_m^\lambda)$, $B_{1i}^\lambda = B_{1i} \lambda_i^{\text{vec}}$, $D_i^\lambda = D_i \lambda_i^{\text{vec}}$, and $\lambda_i^{\text{vec}} = (\lambda_{i1} \ \lambda_{i2} \ \dots \ \lambda_{iv})$, for $i = 1, 2, \dots, m$.

In order to estimate the system order and determine the unknown elements, as are presented in system (3), we use the MOESP algorithm, which is basically defined by the following steps:

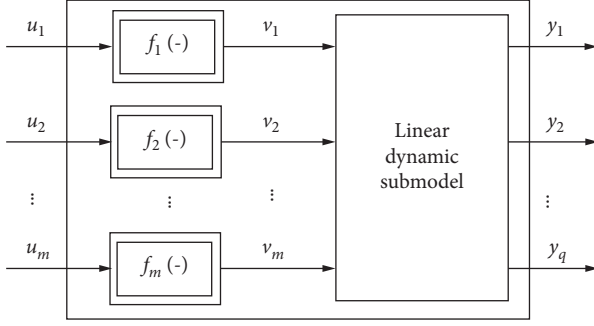


FIGURE 1: Multivariable Hammerstein model configuration.

- (i) Step 1: for sake of simplicity and feasibility, we assume that $\|\lambda_i^{\text{vec}}\|_2 = 1$ and $\lambda_{i1} = 1$, for $i = 1, 2, \dots, m$ [23, 28, 41].
- (ii) Step 2: we determine the estimates \hat{A} , \hat{B}_1^λ , \hat{B}_2^λ , \hat{C} , and \hat{D}^λ of matrices A , B_1^λ , B_2^λ , C , and D^λ directly from the available input-output data.
- (iii) Step 3: we compute a matrix estimate $\hat{\Theta}_i$ of Θ_i , which is defined as

$$\hat{\Theta}_i \triangleq \begin{pmatrix} B_{1i}^\lambda \\ D_i^\lambda \end{pmatrix} = \begin{pmatrix} B_{1i} \\ D_i \end{pmatrix} \lambda_i^{\text{vec}}, \quad (4)$$

by solving the following optimization problem:

$$(\hat{B}_{1i}, \hat{D}_i, \hat{\lambda}_i^{\text{vec}}) = \arg \left(\min_{B_{1i}, D_i, \lambda_i^{\text{vec}}} \left(\left\| \hat{\Theta}_i - \begin{pmatrix} B_{1i} \\ D_i \end{pmatrix} \lambda_i^{\text{vec}} \right\|_2^2 \right) \right). \quad (5)$$

- (iv) Step 4: based on the singular value decomposition (SVD) theorem, as is detailed in [42], we calculate the partition of $\hat{\Theta}_i$ as follows:

$$\hat{\Theta}_i = [U_1 \ U_2] \begin{bmatrix} \Sigma_1 & 0 \\ 0 & \Sigma_2 \end{bmatrix} \begin{bmatrix} V_1^\perp \\ V_2^\perp \end{bmatrix}, \quad (6)$$

where U_1 , V_1 , and Σ_1 are specific matrices of appropriate dimensions.

- (v) Step 5: we compute finally the estimates \hat{B}_{1i} , \hat{D}_i , and $\hat{\lambda}_i^{\text{vec}}$ so that the following system of equations is satisfied:

$$\begin{cases} \begin{bmatrix} \hat{B}_{1i} \\ \hat{D}_i \end{bmatrix} = U_1 \Sigma_1, \\ \hat{\lambda}_i^{\text{vec}} = V_1, \quad \text{for } i = 1, 2, \dots, m. \end{cases} \quad (7)$$

3. Nonfragile H_∞ Control Scheme Design

In this section, we discuss sufficient conditions that guarantee the global asymptotic stability in closed loop of the following system:

$$\begin{cases} x_{k+1} = Ax_k + B_1 V_k + B_2 w_k, \\ z_k = C_z x_k + D_1 V_k + D_2 w_k, \end{cases} \quad (8)$$

where $C_z \in \mathbb{R}^{p \times n}$ is the output matrix of the controlled output vector $z_k \in \mathbb{R}^p$, $D_1 \in \mathbb{R}^{p \times m}$, and $D_2 \in \mathbb{R}^{p \times n}$.

In what follows, we assume that the m -nonlinearities:

$$v_{i,k} = f_i(u_{i,k}) = u_{i,k} + \lambda_{i2} u_{i,k}^2 + \dots + \lambda_{iv} u_{i,k}^v, \quad (9)$$

are not bijective and approximated of the following form:

$$u_{i,k} = f_{i,\text{app}}^{-1}(\hat{v}_{i,k}) = \beta_{i1} \hat{v}_{i,k} + \beta_{i2} \hat{v}_{i,k}^2 + \dots + \beta_{iv} \hat{v}_{i,k}^v + \text{hot}. \quad (10)$$

where (hot) denotes the higher order terms. As the nonlinearities (9) and (10) are in series, we may write

$$v_{i,k} = \psi_i(\hat{v}_{i,k}) = f_i(f_{i,\text{app}}^{-1}(\hat{v}_{i,k})). \quad (11)$$

In addition, the parameters β_{ij} are determined by solving $\hat{v}_i(+\infty) = v_i(+\infty)$, for $i = 1, 2, \dots, m$. An example of calculation for the order $v = 3$ is detailed in Appendix A.

With the above approximation, system (8) is transformed as follows:

$$\begin{cases} x_{k+1} = Ax_k + B_1^\rho \hat{V}_k + B_2 w_k, \\ z_k = C_z x_k + D_1^\rho \hat{V}_k + D_2 w_k, \end{cases} \quad (12)$$

where $B_1^\rho = (B_{11}^{\rho_1} B_{12}^{\rho_2} \dots B_{1m}^{\rho_m})$, $D_1^\rho = (D_{11}^{\rho_1} D_{12}^{\rho_2} \dots D_{1m}^{\rho_m})$, $B_{1i}^{\rho_i} = B_{1i} \rho_{i,k}(\hat{v}_{i,k})$, $D_{1i}^{\rho_i} = D_{1i} \rho_{i,k}(\hat{v}_{i,k})$, for $i = 1, 2, \dots, m$, $\rho_{i,k}(\hat{v}_{i,k}) = \begin{cases} \psi_i(\hat{v}_{i,k})/\hat{v}_{i,k} & \text{if } \hat{v}_{i,k} \neq 0 \\ 1 & \text{else} \end{cases}$, and $\hat{V}_k = (\hat{v}_{1,k} \ \hat{v}_{2,k} \ \dots \ \hat{v}_{m,k})^\perp$.

Using then the polytopic transformation method, the m -nonlinearities $\rho_i(\hat{v}_{i,k})$ are decomposed as follows:

$$\rho_{i,k}(\hat{v}_{i,k}) = H_i^1(\hat{v}_{i,k}) \bar{\sigma}_i + H_i^2(\hat{v}_{i,k}) \underline{\sigma}_i, \quad (13)$$

with

$$H_i^1(\hat{v}_{i,k}) = \frac{\rho_{i,k}(\hat{v}_{i,k}) - \underline{\sigma}_i}{\bar{\sigma}_i - \underline{\sigma}_i}, \quad (14)$$

$$H_i^2(\hat{v}_{i,k}) = 1 - H_i^1(\hat{v}_{i,k}), \quad (15)$$

where $\bar{\sigma}_i$ and $\underline{\sigma}_i$ are the maximum and minimum of $\rho_i(\hat{v}_{i,k})$, respectively.

For the convenience of notations, we define $H_i^j = H_i^j(\hat{v}_{i,k})$, $w_i = w_i(\hat{v}_{j,k})$, and $h_i = h_i(\hat{v}_{j,k})$.

Thereafter, we construct the following fuzzy subsystems:

$$\begin{aligned} \text{rule 1: if } (\hat{v}_{1,k} \text{ is } H_1^1) \text{ and } (\hat{v}_{2,k} \text{ is } H_2^1) \text{ and } \dots \text{ and } (\hat{v}_{m,k} \text{ is } H_m^1), \\ \text{then } x_{k+1} = Ax_k + \tilde{B}_{11} \hat{V}_k + B_2 w_k, z_k \\ = C_z x_k + \tilde{D}_{11} \hat{V}_k + D_2 w_k, \end{aligned} \quad (16)$$

$$\begin{aligned} \text{rule 2: if } (\hat{v}_{1,k} \text{ is } H_1^1) \text{ and } (\hat{v}_{2,k} \text{ is } H_2^2) \text{ and } \dots \text{ and } (\hat{v}_{m,k} \text{ is } H_m^2), \\ \text{then } x_{k+1} = Ax_k + \tilde{B}_{12} \hat{V}_k + B_2 w_k, z_k = C_z x_k + \tilde{D}_{12} \hat{V}_k + D_2 w_k, \\ \vdots \end{aligned} \quad (17)$$

rule $\varsigma = 2^m$: if $(\hat{v}_{1,k}$ is H_1^2) and $(\hat{v}_{2,k}$ is H_2^2)
 and \dots $(\hat{v}_{m,k}$ is H_m^2),
 then $x_{k+1} = Ax_k + \tilde{B}_{1\varsigma}\hat{V}_k + B_2w_k, z_k$
 $= C_zx_k + \tilde{D}_{1\varsigma}\hat{V}_k + D_2w_k,$

where $\tilde{B}_{11} = (\tilde{B}_{11}^{\rho_1} \tilde{B}_{12}^{\rho_2} \dots \tilde{B}_{1m}^{\rho_m}), \tilde{D}_{11} = (\tilde{D}_{11}^{\rho_1} \tilde{D}_{12}^{\rho_2} \dots \tilde{D}_{1m}^{\rho_m}),$
 $\tilde{B}_{12} = (\tilde{B}_{11}^{\rho_1} \tilde{B}_{12}^{\rho_2} \dots \tilde{B}_{1m}^{\rho_m}), \tilde{D}_{12} = (\tilde{D}_{11}^{\rho_1} \tilde{D}_{12}^{\rho_2} \dots \tilde{D}_{1m}^{\rho_m}),$
 $\tilde{B}_{1\varsigma} = (\tilde{B}_{11}^{\rho_1} \tilde{B}_{12}^{\rho_2} \dots \tilde{B}_{1m}^{\rho_m}), \tilde{D}_{1\varsigma} = (\tilde{D}_{11}^{\rho_1} \tilde{D}_{12}^{\rho_2} \dots \tilde{D}_{1m}^{\rho_m}),$
 $\tilde{B}_{1i}^{\rho_i} = \bar{\sigma}_i B_{1i}, \tilde{D}_{1i}^{\rho_i} = \bar{\sigma}_i D_{1i},$ and $\tilde{D}_{1i}^{\rho_i} = \underline{\sigma}_i D_{1i},$ for $i = 1, 2, \dots, m.$
 As a consequence, the final system is inferred as follows:

$$\begin{cases} x_{k+1} = \sum_{i=1}^{\varsigma} h_i (Ax_k + \tilde{B}_{1i}\hat{V}_k + B_2w_k), \\ z_k = \sum_{i=1}^{\varsigma} h_i (C_zx_k + \tilde{D}_{1i}\hat{V}_k + D_2w_k), \end{cases} \quad (19)$$

where the nonlinear weighting functions are $h_i = w_i / \sum_{i=1}^{\varsigma} w_i,$ such that $0 \leq h_i \leq 1$ and $\sum_{i=1}^{\varsigma} h_i = 1,$ and

$$\begin{cases} w_1 = H_1^1 H_2^1 \dots H_m^1, \\ w_2 = H_1^1 H_2^1 \dots H_m^1, \\ \vdots \\ w_{\varsigma} = H_1^2 H_2^2 \dots H_m^2. \end{cases} \quad (20)$$

For stabilizing system (19) in closed loop, we assume that each subsystem (A, \tilde{B}_{1i}) is fully controllable and measurable. Then, we use the nonfragile control law:

$$\hat{V}_k = -\bar{K}x_k, \quad (21)$$

with the uncertainty:

$$\bar{K} = K + \Delta K = (I + \mu\phi_k)K, \quad (22)$$

where $K \in \mathbb{R}^{m \times n}$ is the nominal controller, $\mu > 0$ is a scalar to be assigned, $I \in \mathbb{R}^{m \times m}$ denotes the identity matrix, and $\phi_k \in \mathbb{R}^{m \times m},$ such that $\phi_k^{\perp} \phi_k \leq I.$

Substituting (21) into (19), we obtain the final controlled system:

$$\begin{cases} x_{k+1} = \sum_{i=1}^{\varsigma} h_i (\bar{G}_i x_k + B_2 w_k), \\ z_k = \sum_{i=1}^{\varsigma} h_i (\bar{F}_i x_k + D_2 w_k), \end{cases} \quad (23)$$

where $\bar{G}_i = G_i + \Delta G_i, \bar{F}_i = F_i + \Delta F_i, G_i = A - \tilde{B}_{1i}K,$
 $\Delta G_i = -\mu \tilde{B}_{1i} \phi_k K, F_i = C_z - \tilde{D}_{1i}K,$ and $\Delta F_i = -\mu \tilde{D}_{1i} \phi_k K.$

The closed-loop system (23) is globally asymptotically stable with decay rate α and achieves a prescribed attenuation level γ if

$$\|T_{zw}\|_{\infty} = \sup_{\|w\|_2 \neq 0} \frac{\|z\|_2}{\|w\|_2} < \gamma. \quad (24)$$

As a consequence, we announce the following theorem.

Theorem 1. *The equilibrium $(x = 0_{\mathbb{R}^n})$ of the closed-loop system (23) is quadratically and globally asymptotically stable with decay rate α satisfying the control performance objective (24) if there exist positive scalars $\mu, \tau_1, \tau_2, \delta_{12} = \tau_1^{-1} + \tau_2^{-1},$ and $\beta \in]0, 1[,$ a common symmetric positive definite matrix $X \in \mathbb{R}^{n \times n},$ and $M \in \mathbb{R}^{m \times n}$ verifying the following LMI formulation:*

$$\begin{aligned} & \text{minimize } \beta \\ & \text{subject to : } \begin{pmatrix} -\beta X & * & * & * & * \\ 0 & -\gamma^2 I & * & * & * \\ AX - \tilde{B}_{1i}M & B_2 & -\ell_{33,i} & * & * \\ C_z X - \tilde{D}_{1i}M & D_2 & 0 & -\ell_{44,i} & * \\ M & 0 & 0 & 0 & -\delta_{12}^{-1} I \end{pmatrix} < 0, \end{aligned} \quad (25)$$

for $i = 1, 2, \dots, \varsigma,$ where $\ell_{33,i} = X - \tau_1 \mu^2 \tilde{B}_{1i} \tilde{B}_{1i}^{\perp}$ and $\ell_{44,i} = I - \tau_2 \mu^2 \tilde{D}_{1i} \tilde{D}_{1i}^{\perp}.$

Then, the feedback gain $K,$ as is shown in (22), is calculated by using the following relation:

$$K = MX^{-1}. \quad (26)$$

Proof. The controlled system (23) is globally asymptotically stable with decay rate α if there exist a discrete-time quadratic Lyapunov function $V_{\text{Lyap}}(x_k) = x_k^{\perp} P x_k > 0$ and a positive scalar $0 < \alpha < 1$ such that

$$\Delta V_{\text{Lyap}}(x_k) \leq (\alpha^2 - 1) V_{\text{Lyap}}(x_k), \quad (27)$$

where $\Delta V_{\text{Lyap}}(x_k) = V_{\text{Lyap}}(x_{k+1}) - V_{\text{Lyap}}(x_k)$ and $P \in \mathbb{R}^{n \times n}$ is a symmetric positive definite matrix. By considering (27) in (24), we may write

$$\Delta V_{\text{Lyap}}(x_k) - (\alpha^2 - 1) V_{\text{Lyap}}(x_k) + z_k^{\perp} z_k - \gamma^2 w_k^{\perp} w_k < 0. \quad (28)$$

By, respectively, substituting the dynamics of x_{k+1} and z_k into (28), it becomes

$$\sum_{i=1}^{\varsigma} h_i \begin{pmatrix} x_k \\ w_k \end{pmatrix}^{\perp} \Gamma_i \begin{pmatrix} x_k \\ w_k \end{pmatrix} < 0, \quad (29)$$

where $\Gamma_i = \begin{pmatrix} \bar{G}_i^{\perp} P \bar{G}_i - \alpha^2 P + \bar{F}_i^{\perp} \bar{F}_i & * \\ B_2^{\perp} P \bar{G}_i + D_2^{\perp} D_2 & B_2^{\perp} P B_2 + D_2^{\perp} D_2 - \gamma^2 I \end{pmatrix}$
 and the symbol $(*)$ represents the transposed element in the symmetric position.

As the nonlinear functions $h_i \in [0, 1],$ matrix inequality (29) is equivalent to $\Gamma_i < 0,$ for $i = 1, 2, \dots, \varsigma.$ Using the Schur Complement, as is presented in Appendix B, we get

$$\begin{pmatrix} -\alpha^2 P & * & * & * \\ 0 & -\gamma^2 I & * & * \\ P \bar{G}_i & P B_2 & -P & * \\ \bar{F}_i & D_2 & 0 & -I \end{pmatrix} < 0. \quad (30)$$

Denoting $X = P^{-1}$, $M = KX$, and $\beta = \alpha^2$ and, respectively, premultiplying and postmultiplying (30) by positive definite matrix $\text{diag}(X, I, X, I)$ yields

$$\begin{pmatrix} -\beta X & * & * & * \\ 0 & -\gamma^2 I & * & * \\ \bar{G}_i X & B_2 & -X & * \\ \bar{F}_i X & D_2 & 0 & -I \end{pmatrix} < 0. \quad (31)$$

As the above matrix inequality contains certain terms $\Psi_{i,k}$ and uncertain ones $\Delta\Psi_{i,k}$, (31) can be transformed as follows:

$$\Psi_{i,k} + \Delta\Psi_{i,k} < 0, \quad (32)$$

with

$$\Psi_{i,k} = \begin{pmatrix} -\beta X & * & * & * \\ 0 & -\gamma^2 I & * & * \\ G_i X & B_2 & -X & * \\ F_i X & D_2 & 0 & -I \end{pmatrix}, \quad (33)$$

$$\Delta\Psi_{i,k} = \begin{pmatrix} 0 & 0 & * & * \\ 0 & 0 & 0 & 0 \\ -\mu \tilde{B}_{1i} \phi_k M & 0 & 0 & 0 \\ -\mu \tilde{D}_{1i} \phi_k M & 0 & 0 & 0 \end{pmatrix}. \quad (34)$$

We notice that there are antidiagonal terms in $\Delta\Psi_{i,k}$. However, we use the Separation Lemma, as is defined in Appendix C, to transform them into diagonal terms as follows:

$$\Delta\Psi_{i,k} \leq \begin{pmatrix} \delta_{12} M^\perp M & 0 & 0 & 0 \\ 0 & 0 & 0 & 0 \\ 0 & 0 & \tau_1 \mu^2 \tilde{B}_{1i} \tilde{B}_{1i}^\perp & 0 \\ 0 & 0 & 0 & \tau_2 \mu^2 \tilde{D}_{1i} \tilde{D}_{1i}^\perp \end{pmatrix}, \quad (35)$$

where τ_1 , τ_2 , and $\delta_{12} = \tau_1^{-1} + \tau_2^{-1}$ are positive scalars to be assigned.

Referring to relations (33) and (35), we obtain

$$\begin{pmatrix} -\beta X + \delta_{12} M^\perp M & * & * & * \\ 0 & -\gamma^2 I & * & * \\ G_i X & B_2 & -X + \tau_1 \mu^2 \tilde{B}_{1i} \tilde{B}_{1i}^\perp & * \\ F_i X & D_2 & 0 & -I + \tau_2 \mu^2 \tilde{D}_{1i} \tilde{D}_{1i}^\perp \end{pmatrix} < 0. \quad (36)$$

After some manipulations, we get the LMI formulation (25). \square

Remark 1. Consider system (19) with no uncertainty, i.e., $\Delta K = 0$. Then, the origin of the closed-loop system (26) is globally asymptotically stable if [27]

$$\begin{aligned} & \underset{X,R,\gamma}{\text{minimize}} \beta \\ & \text{subject to:} \quad \begin{pmatrix} -\beta X & * & * & * \\ 0 & -\gamma^2 I & * & * \\ AX - \tilde{B}_{1i} M & B_2 & -X & * \\ C_z X - \tilde{D}_{1i} M & D_2 & 0 & -I \end{pmatrix} < 0, \quad \text{for } i = 1, 2, \dots, \varsigma. \end{pmatrix} \quad (37) \end{aligned}$$

In the following, a numerical example is provided to demonstrate the validity and the effectiveness of the proposed control scheme.

4. Application to a TRMS

The objective of this simulation study is to stabilize the controlled TRMS and its identified multivariable

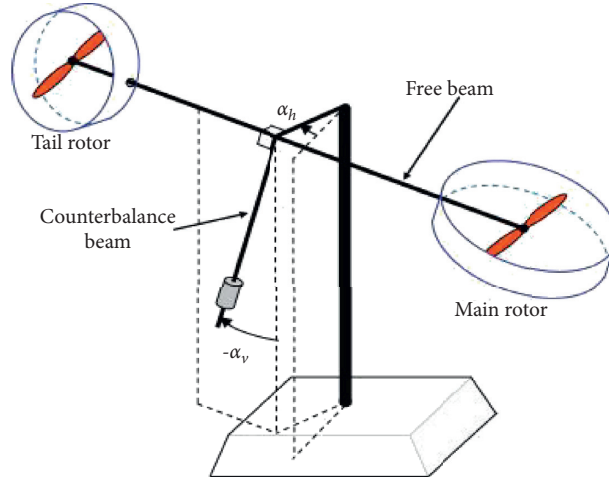


FIGURE 2: TRMS [43].

Hammerstein model at the origin, as an asymptotically stable equilibrium point. More precisely, its system behaviour resembles that of a helicopter, as is seen in Figure 2. It consists of two rotors (main and tail), which are situated on a beam together with a counterbalance. The inputs of the open-loop system are the voltages u_1 (V) and u_2 (V) applied, respectively, to the main and tail rotors. The first output is called pitch angle y_1 (rad) when the main rotor is free to rotate in the horizontal plane. The second output is called yaw angle y_2 (rad) when the tail rotor is free to rotate in the vertical plane.

The studied system is described by the following continuous-time nonlinear equations [43]:

$$\begin{cases} I_1 \ddot{\psi} = M_1 - M_{FG} - M_{B\psi} - M_G, \\ I_2 \ddot{\phi} = M_2 - M_{B\phi} - M_R, \end{cases} \quad (38)$$

where $M_1 = a_1 \eta_1^2 + b_1 \eta_1$, $M_{FG} = M_g \sin(\psi)$, $M_{B\psi} = B_1 \psi \dot{\psi}$, $M_G = K_{gy} M_1 \dot{\phi} \cos(\psi) - K_{gx} \dot{\phi}^2 \sin(2\psi)$, $M_2 = a_2 \eta_2^2 + b_2 \eta_2$, $M_{B\phi} = B_1 \phi \dot{\phi}$, $\dot{\eta}_1 = -T_{10}/T_{11} \eta_1 + k_1/T_{11} u_1$, $\dot{\eta}_2 = -T_{20}/T_{21} \eta_2 + k_2/T_{21} u_2$, $M_R = k_c \eta_1 + T_0 s + T_p s$, and s is the Laplace variable. All parameters are defined in Appendix D.

4.1. Identification Result. From an identification point of view, we assume that the input-output data are available. Then, we consider that the sampling period is $T = 0.1$ s and the inputs are $u_{1,k} = 2.5 \sin(0.6\pi kT)$ and $u_{2,k} = 2 \sin(0.8\pi kT)$. Figures 3 and 4 depict the responses of the true (solid line) and estimated (dashed line) outputs of the open-loop system.

It is then clear that the nonlinear TRMS is accurately identified by 2-input 2-output Hammerstein state-space model, which is described by

$$\begin{cases} x_{k+1} = Ax_k + B_1 V_k + B_2 w_k, \\ Y_k = Cx_k + DV_k + \varepsilon_k, \\ v_{1,k} = u_{1,k} + 0.0381u_{1,k}^2 - 0.0457u_{1,k}^3, \\ v_{2,k} = u_{2,k} + 0.0237u_{2,k}^2 - 0.0118u_{2,k}^3, \end{cases} \quad (39)$$

where

$$x_k = \begin{pmatrix} x_{1,k} \\ x_{2,k} \\ x_{3,k} \\ x_{4,k} \end{pmatrix}, V_k = \begin{pmatrix} v_{1,k} \\ v_{2,k} \end{pmatrix}, Y_k = \begin{pmatrix} y_{1,k} \\ y_{2,k} \end{pmatrix}, w_k \in \mathbb{R}^4, \varepsilon_k \in \mathbb{R}^2,$$

$$A = \begin{pmatrix} 0.9709 & -0.3380 & 0.1232 & 0.0306 \\ 0.1179 & 0.9745 & 0.0093 & -0.0109 \\ -0.0375 & 0.0087 & 0.9974 & -0.0798 \\ 0.0109 & -0.0226 & 0.0270 & 0.8693 \end{pmatrix},$$

$$B_1 = \begin{pmatrix} 0.0111 & 0.0547 \\ -0.0131 & -0.0027 \\ 0.2172 & 0.3044 \\ 0.0865 & 0.0520 \end{pmatrix},$$

$$B_2 = \begin{pmatrix} -0.2292 & 0.5655 & 7.7293 & 0.2978 \\ 1.4445 & 0.2131 & -5.6435 & 0.0878 \\ -0.4621 & -0.0928 & -2.4361 & 0.1226 \\ -0.2324 & 0.0914 & 9.9696 & -0.7869 \end{pmatrix},$$

$$C = \begin{pmatrix} -0.0853 & 0.2915 & -0.1147 & 0.0093 \\ 0.0121 & -0.1440 & -0.3784 & -0.1127 \end{pmatrix},$$

$$D = \begin{pmatrix} -0.0326 & 0.0063 \\ 0.0284 & -0.0713 \end{pmatrix}. \quad (40)$$

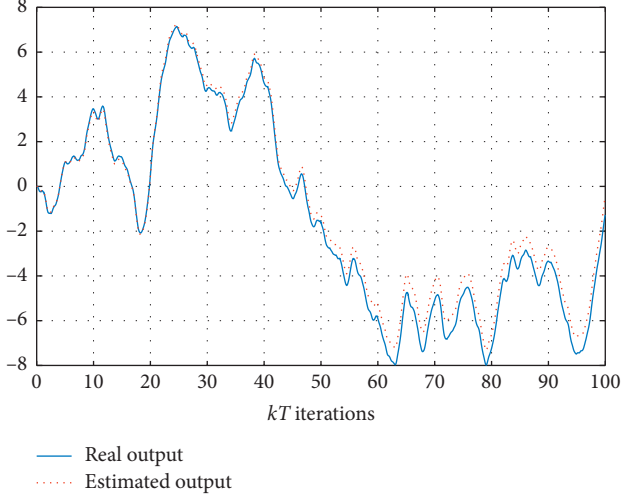


FIGURE 3: Response of the pitch angle of the open-loop system.

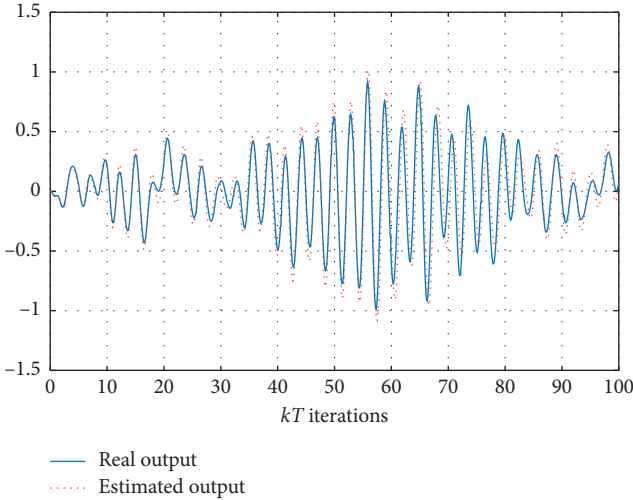


FIGURE 4: Response of the yaw angle of the open-loop system.

4.2. Control Results. From a control point of view, we assume that the inverse functions $u_{i,k} = f_{i,\text{app}}^{-1}(\hat{v}_{i,k})$, for $i = \{1, 2\}$, are approximated as follows:

$$\begin{cases} u_{1,k} = \hat{v}_{1,k} - 0.0381\hat{v}_{1,k}^2 + 0.1219\hat{v}_{1,k}^3 + \text{hot}, \\ u_{2,k} = \hat{v}_{2,k} - 0.0237\hat{v}_{2,k}^2 + 0.0592\hat{v}_{2,k}^3 + \text{hot}. \end{cases} \quad (41)$$

Choosing the scalars $\underline{\sigma}_1 = 0.4$, $\bar{\sigma}_1 = 1.7$, $\underline{\sigma}_2 = 0.3$, and $\bar{\sigma}_2 = 2$, Figure 5 depicts the evolution of nonlinearities $v_{i,k} = \psi_i(\hat{v}_{i,k})$, for $i = \{1, 2\}$. This leads to obtain, for the control scheme, the bounded control signals $\hat{v}_{1,k} \in [-5.87, 5.73]$ and $\hat{v}_{2,k} \in [-2.33, 2.24]$.

Afterwards, we assume that the controlled output z_k is expressed by

$$z_k = C_z x_k + D_1 V_k + D_2 w_k, \quad (42)$$

where $z_k = \begin{pmatrix} z_{1,k} \\ z_{2,k} \end{pmatrix}$, $C_z = C$, $D_1 = D$, and $D_2 = \begin{pmatrix} 1 & 0 & 0 & 0 \\ 0 & 0 & 1 & 0 \end{pmatrix}$.

By considering the pairs $(\bar{\sigma}_1, \bar{\sigma}_2)$, $(\bar{\sigma}_1, \underline{\sigma}_2)$, $(\underline{\sigma}_1, \bar{\sigma}_2)$, and $(\underline{\sigma}_1, \underline{\sigma}_2)$, we construct the following fuzzy subsystems:

$$\begin{aligned} \text{rule 1: if } (\hat{v}_{1,k} \text{ is } H_1^1) \text{ and } (\hat{v}_{2,k} \text{ is } H_2^1), \\ \text{then } x_{k+1} = Ax_k + \tilde{B}_{11}\hat{V}_k + B_2 w_k, z_k \\ = C_z x_k + \tilde{D}_{11}\hat{V}_k + D_2 w_k, \end{aligned} \quad (43)$$

$$\begin{aligned} \text{rule 2: if } (\hat{v}_{1,k} \text{ is } H_1^1) \text{ and } (\hat{v}_{2,k} \text{ is } H_2^2), \\ \text{then } x_{k+1} = Ax_k + \tilde{B}_{12}\hat{V}_k + B_2 w_k, z_k \\ = C_z x_k + \tilde{D}_{12}\hat{V}_k + D_2 w_k, \end{aligned} \quad (44)$$

$$\begin{aligned} \text{rule 3: if } (\hat{v}_{1,k} \text{ is } H_1^2) \text{ and } (\hat{v}_{2,k} \text{ is } H_2^1), \\ \text{then } x_{k+1} = Ax_k + \tilde{B}_{13}\hat{V}_k + B_2 w_k, z_k \\ = C_z x_k + \tilde{D}_{13}\hat{V}_k + D_2 w_k, \end{aligned} \quad (45)$$

$$\begin{aligned} \text{rule 4: if } (\hat{v}_{1,k} \text{ is } H_1^2) \text{ and } (\hat{v}_{2,k} \text{ is } H_2^2), \\ \text{then } x_{k+1} = Ax_k + \tilde{B}_{14}\hat{V}_k + B_2 w_k, z_k \\ = C_z x_k + \tilde{D}_{14}\hat{V}_k + D_2 w_k, \end{aligned} \quad (46)$$

where

$$\begin{aligned} \tilde{B}_{11} = \begin{pmatrix} 0.0187 & 0.1094 \\ -0.0223 & -0.0054 \\ 0.3692 & 0.6088 \\ 0.1470 & 0.1040 \end{pmatrix}, \tilde{B}_{12} = \begin{pmatrix} 0.0187 & 0.0164 \\ -0.0223 & -0.0008 \\ 0.3692 & 0.0913 \\ 0.1470 & 0.0156 \end{pmatrix}, \\ \tilde{B}_{13} = \begin{pmatrix} 0.0044 & 0.1094 \\ -0.0052 & -0.0054 \\ 0.0869 & 0.6088 \\ 0.0346 & 0.1040 \end{pmatrix}, \tilde{B}_{14} = \begin{pmatrix} 0.0044 & 0.0164 \\ -0.0052 & -0.0008 \\ 0.0869 & 0.0913 \\ 0.0346 & 0.0156 \end{pmatrix}, \\ \tilde{D}_{11} = \begin{pmatrix} -0.0554 & 0.0126 \\ 0.0483 & -0.1426 \end{pmatrix}, \tilde{D}_{12} = \begin{pmatrix} -0.0554 & 0.0019 \\ 0.0483 & -0.0214 \end{pmatrix}, \\ \tilde{D}_{13} = \begin{pmatrix} -0.0130 & 0.0126 \\ 0.0114 & -0.1426 \end{pmatrix}, \tilde{D}_{14} = \begin{pmatrix} -0.0130 & 0.0019 \\ 0.0114 & -0.0214 \end{pmatrix}. \end{aligned} \quad (47)$$

As the pairs (A, \tilde{B}_{1i}) , for $i = \{1, 2, 3, 4\}$, are controllable, the resulting fuzzy system can be described as follows:

$$\begin{cases} x_{k+1} = \sum_{i=1}^4 h_i (Ax_k + \tilde{B}_{1i}\hat{V}_k + B_2 w_k), \\ z_k = \sum_{i=1}^4 h_i (C_z x_k + \tilde{D}_{1i}\hat{V}_k + D_2 w_k), \end{cases} \quad (48)$$

where the nonlinear weighting functions $h_i = w_i / \sum_{i=1}^4 w_i$ are depicted in Figure 6.

Using the LMI formulation (25) with $\mu = 0.85$ and $\gamma = 0.7$, we obtain $\alpha = 0.794$, $\beta = 0.63$, and

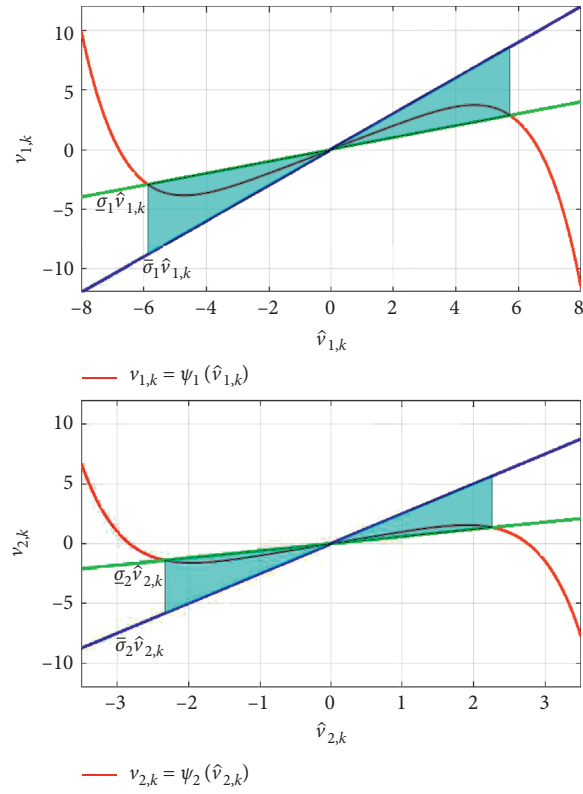


FIGURE 5: Evolution of nonlinear functions. Up Polt: $v_{1,k} = \psi_1(\hat{v}_{1,k})$. Down Polt: $v_{2,k} = \psi_2(\hat{v}_{2,k})$.

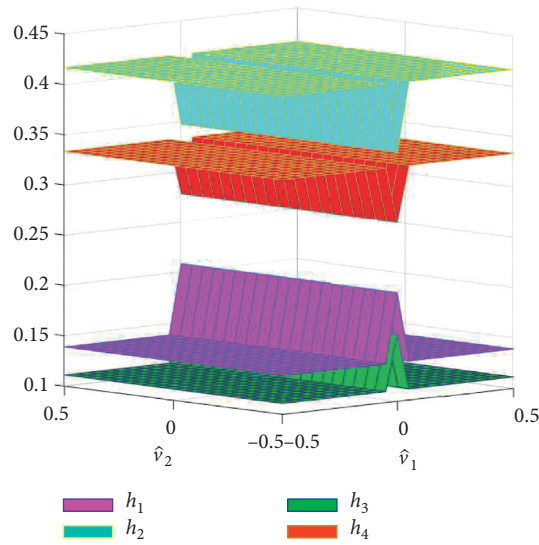


FIGURE 6: Weighting functions for the four fuzzy sets considered.

$$P = \begin{pmatrix} 6.4497 & 0.8651 & -0.2691 & 0.1327 \\ 0.8651 & 4.7781 & -0.3205 & 0.1191 \\ -0.2691 & -0.3205 & 5.0222 & 0.4860 \\ 0.1327 & 0.1191 & 0.4860 & 4.9015 \end{pmatrix}, \quad (49)$$

$$K = \begin{pmatrix} -0.5072 & -0.2251 & 2.3094 & 1.4059 \\ 0.5327 & -0.0653 & 1.4641 & -0.4069 \end{pmatrix}.$$

Hence, by considering the nonfragile control law (21) subject to the uncertainty (22) with $\phi_k = \begin{pmatrix} 0.5 \sin(\pi k) & 0 \\ 0 & 0.5 \cos(\pi k) \end{pmatrix}$, the inferred controlled system can be described as follows:

$$\begin{cases} x_{k+1} = \sum_{i=1}^4 h_i (\bar{G}_i x_k + B_2 w_k), \\ z_k = \sum_{i=1}^4 h_i (\bar{F}_i x_k + D_2 w_k), \end{cases} \quad (50)$$

where $\bar{G}_i = G_i + \Delta G_i$, $\bar{F}_i = F_i + \Delta F_i$, $\Delta G_i = -\mu \bar{B}_{1i} \phi_k K$, $\Delta F_i = -\mu \bar{D}_{1i} \phi_k K$, for $i \in \{1, 2, 3, 4\}$, and

$$G_1 = \begin{pmatrix} 0.9221 & -0.3266 & -0.0802 & 0.0488 \\ 0.1095 & 0.9691 & 0.0686 & 0.0182 \\ -0.1745 & 0.1316 & -0.7467 & -0.3512 \\ 0.0301 & 0.0173 & -0.4649 & 0.7049 \end{pmatrix},$$

$$G_2 = \begin{pmatrix} 0.9716 & -0.3327 & 0.0560 & 0.0110 \\ 0.1070 & 0.9694 & 0.0619 & 0.0201 \\ 0.1011 & 0.0978 & 0.0110 & -0.5618 \\ 0.0772 & 0.0115 & -0.3354 & 0.6689 \end{pmatrix},$$

$$G_3 = \begin{pmatrix} 0.9149 & -0.3299 & -0.0471 & 0.0689 \\ 0.1181 & 0.9730 & 0.0293 & -0.0057 \\ -0.3177 & 0.0680 & -0.0946 & 0.0458 \\ -0.0269 & -0.0080 & -0.2052 & 0.8630 \end{pmatrix},$$

$$G_4 = \begin{pmatrix} 0.9644 & -0.3359 & 0.0890 & 0.0311 \\ 0.1157 & 0.9733 & 0.0226 & -0.0039 \\ -0.0421 & 0.0342 & 0.6631 & -0.1648 \\ 0.0201 & -0.0138 & -0.0757 & 0.8270 \end{pmatrix},$$

$$F_1 = \begin{pmatrix} -0.1201 & 0.2798 & -0.0052 & 0.0923 \\ 0.1125 & -0.1425 & -0.2811 & -0.2386 \end{pmatrix},$$

$$F_2 = \begin{pmatrix} -0.1144 & 0.2791 & 0.0105 & 0.0880 \\ 0.0480 & -0.1345 & -0.4586 & -0.1893 \end{pmatrix},$$

$$F_3 = \begin{pmatrix} -0.0986 & 0.2894 & -0.1030 & 0.0328 \\ 0.0938 & -0.1508 & -0.1959 & -0.1867 \end{pmatrix},$$

$$F_4 = \begin{pmatrix} -0.0929 & 0.2887 & -0.0874 & 0.0284 \\ 0.0293 & -0.1428 & -0.3733 & -0.1374 \end{pmatrix}. \quad (51)$$

$$(52)$$

Figures 7–10 show the simulation results of applying the designed nonfragile H_∞ controller to the TRMS (dashed line) and its identified Hammerstein model (solid line) with null

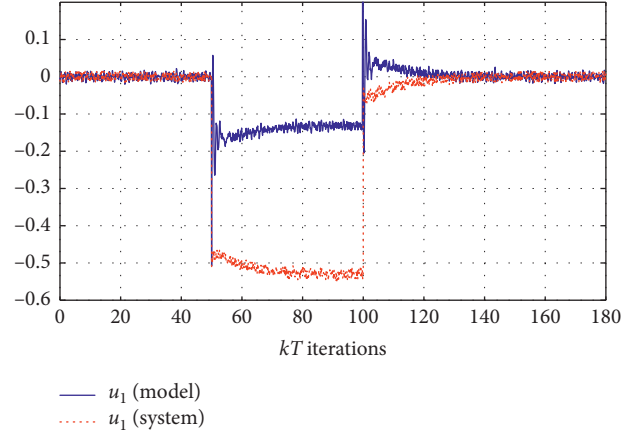


FIGURE 7: Control signal u_1 (V).

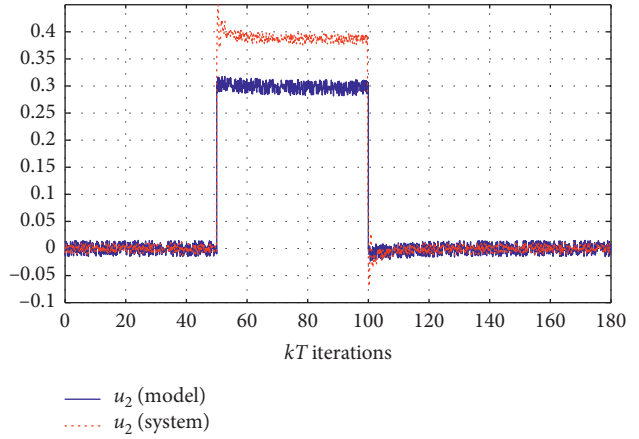


FIGURE 8: Control signal u_2 (V).

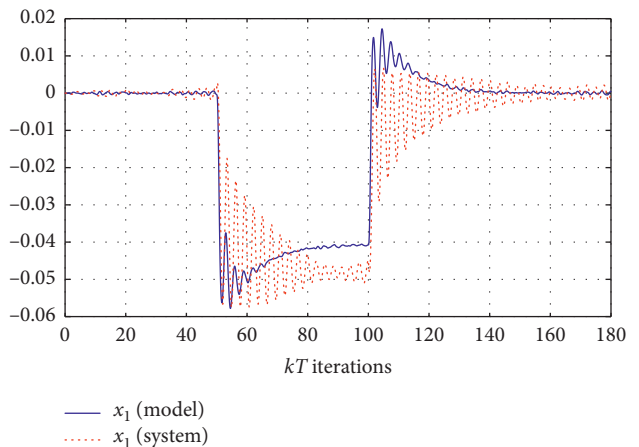


FIGURE 9: Response of the pitch angle of the closed-loop system.

initial conditions and the exogenous disturbance signal $w_k = (\text{rand } 0 \text{ rand } 0)^+$, where (rand) is a uniform number with a uniform distribution on the interval $[0, 0.01]$, which is added by $w_k^+ = -0.15$ if $50 \leq kT \leq 100$ and 0 otherwise.

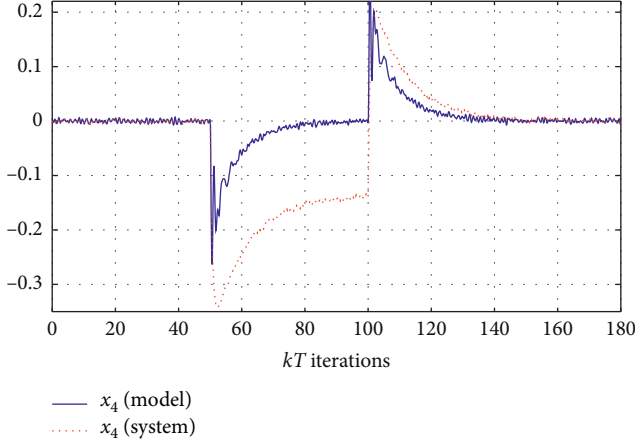


FIGURE 10: Response of the yaw angle of the closed-loop system.

The obtained results indicate that the designed robust and nonfragile H_∞ controller shows good results. However, the responses of the pitch and yaw angles of the controlled nonlinear system and its identified Hammerstein model can rapidly achieve the origin despite the presence of external disturbances and uncertainty in the control law.

5. Conclusion

In this paper, a nonfragile H_∞ feedback controller was designed for nonlinear systems described as multivariable Hammerstein model with separate nonlinearities. The parameters of the linear and nonlinear blocks characterizing the multivariable Hammerstein model structure were separately estimated using the MOESP identification algorithm. Unlike the normal control scheme, the inverses of the static nonlinearities were supposed not bijective and approximated by polynomial functions. The T-S fuzzy representation was used to simplify the nonlinear system description and reject the nonlinearity effect in the controller design. Based on the quadratic Lyapunov function and H_∞ criterion, robust H_∞ was then proposed to robustly stabilize the controlled nonlinear system and its identified Hammerstein model and guarantee the attenuation of disturbance effect in spite of controller gain variations. A TRMS was considered to illustrate the validity and the effectiveness of the designed stabilization scheme.

Appendix

A. Calculation of β_{ij} Scalars

The calculation of $\beta_{i,j}$ scalars are presented for $v = 3$. Then, we have

$$\begin{cases} v_{i,k} = f_i(u_{i,k}) = u_{i,k} + \lambda_{i2}u_{i,k}^2 + \lambda_{i3}u_{i,k}^3, \\ u_{i,k} = f_{i,\text{app}}^{-1}(\hat{v}_{i,k}) = \beta_{i1}\hat{v}_{i,k} + \beta_{i2}\hat{v}_{i,k}^2 + \beta_{i3}\hat{v}_{i,k}^3 + \text{hot.} \end{cases} \quad (\text{A.1})$$

Substituting the above quantities, we get

TABLE 1: TRMS parameters.

Symbol	Definition
u_1, u_2	Input signals
ψ	Pitch angle of the beam
ϕ	Yaw angle of the beam
I_1, I_2	Moment of inertia of vertical (horizontal) rotor
M_{FG}	Gravity momentum
$M_{B\psi}, M_{B\phi}$	Friction momentum forces
M_G	Gyroscopic momentum
a_i, b_i	Static parameters of motor i , $i = \{1, 2\}$
M_g	Gravity momentum
$B_{1\psi}, B_{1\phi}$	Friction momentums
K_{gy}, K_{gx}	Gyroscopic momentums
k_{ii}	Motor i gain
T_{i1}, T_{i0}	Motor i denominator
M_R	Cross reaction momentum approximation
k_c	Cross reaction momentum gain
T_p	Cross reaction momentum

$$\begin{aligned} u_{i,k} = f_{i,\text{app}}^{-1}(\hat{v}_{i,k}) \approx & \beta_{i1}(u_{i,k} + \lambda_{i2}u_{i,k}^2 + \lambda_{i3}u_{i,k}^3) \\ & + \beta_{i2}(u_{i,k} + \lambda_{i2}u_{i,k}^2 + \lambda_{i3}u_{i,k}^3)^2 + \beta_{i3}(u_{i,k} + \lambda_{i2}u_{i,k}^2 + \lambda_{i3}u_{i,k}^3)^3. \end{aligned} \quad (\text{A.2})$$

Then, we eliminate the powers higher than 3 of $u_{i,k}$. So, we get

$$\begin{aligned} u_{i,k} = & \beta_{i1}u_{i,k} + (\beta_{i1} + \beta_{i2}\lambda_{i2})u_{i,k}^2 \\ & + (\beta_{i1}\lambda_{i3} + 2\beta_{i2}\lambda_{i2} + \beta_{i3})u_{i,k}^3 + \text{hot.} \end{aligned} \quad (\text{A.3})$$

We obtain finally $\beta_{i1} = 1$, $\beta_{i2} = -\lambda_{i2}$, and $\beta_{i3} = 2\lambda_{i2}^2 - \lambda_{i3}$.

B. Schur Complement

For matrices M , L , and Q with appropriate dimensions, the matrix inequality $\begin{pmatrix} M & * \\ L & Q \end{pmatrix} < 0$ is equal to (i) $Q < 0$, $M - L^+Q^{-1}L < 0$ and (ii) $M < 0$, $Q - LM^{-1}L^+ < 0$ where M and Q are invertible and symmetric.

C. Separation Lemma

For matrices A and B with appropriate dimensions and positive scalars τ , one has $A^+B + B^+A \leq \tau A^+A + \tau^{-1}B^+B$.

D. TRMS Parameters

TRMS parameters are shown in Table 1.

Data Availability

No data were used to support this study.

Conflicts of Interest

The authors declare that there are no conflicts of interest regarding the publication of this paper.

References

- [1] T. Takagi and M. Sugeno, "Fuzzy identification of systems and its applications to modeling and control," *IEEE Transactions on Systems, Man, and Cybernetics*, vol. 15, no. 1, pp. 116–132, 1985.
- [2] K. Tanaka and M. Sugeno, "Stability analysis and design of fuzzy control systems," *Fuzzy Sets and Systems*, vol. 45, no. 2, pp. 135–156, 1992.
- [3] N. Vafamand, S. Khorshidi, and A. Khayatian, "Secure communication for non-ideal channel via robust ts fuzzy observer-based hyperchaotic synchronization," *Chaos, Solitons & Fractals*, vol. 112, pp. 116–124, 2018.
- [4] N. Vafamand, "Transient performance improvement of Takagi-Sugeno fuzzy systems by modified non-parallel distributed compensation controller," *Asian Journal of Control*, 2020.
- [5] G. Mzyk, M. Biegański, and B. Kozdraś, "Multistage identification of an NLN Hammerstein-Wiener system," in *Proceedings of the 22nd International Conference on Methods and Models in Automation and Robotics*, pp. 343–346, IEEE, Miedzyzdroje, Poland, August 2017.
- [6] E. W. Bai, "Frequency domain identification of Hammerstein models," *IEEE Transactions on Automatic Control*, vol. 48, no. 4, pp. 530–542, 2003.
- [7] M.-R. Rahmani and M. Farrokhi, "Fractional-order Hammerstein state-space modeling of nonlinear dynamic systems from input-output measurements," *ISA Transactions*, vol. 96, pp. 177–184, 2020.
- [8] Y. Zhu, "Robust PID tuning using closed-loop identification," *IFAC Proceedings Volumes*, vol. 37, no. 1, pp. 161–166, 2004.
- [9] M. Sadabadi, M. Karrari, and O. Malik, "Nonlinear identification of synchronous generator using Hammerstein model with piecewise linear static maps," *IEEE Lausanne Power Tech*, pp. 1067–1071, Article ID 2272601, 2007.
- [10] R. K. Pearson and M. Pottmann, "Gray-box identification of block-oriented nonlinear models," *Journal of Process Control*, vol. 10, no. 4, pp. 301–315, 2000.
- [11] I. W. Hunter and M. J. Korenberg, "The identification of nonlinear biological systems: Wiener and Hammerstein cascade models," *Biological Cybernetics*, vol. 55, no. 2-3, pp. 135–144, 1986.
- [12] B. Satpati, C. Koley, P. Bhowmik, and S. Datta, "Nonlinear Hammerstein-Hammerstein identification of air preheating furnace of a pneumatic conveying and drying process," in *Proceedings of the 2014 IEEE Conference on Control Applications (CCA)*, pp. 397–402, IEEE, Juan Les Antibes, France, October 2014.
- [13] Y. Liu and E.-W. Bai, "Iterative identification of Hammerstein systems," *Automatica*, vol. 43, no. 2, pp. 346–354, 2007.
- [14] F. Ding and T. Chen, "Identification of Hammerstein nonlinear ARMAX systems," *Automatica*, vol. 41, no. 9, pp. 1479–1489, 2005.
- [15] T. C. Hsia, "A multi-stage least squares method for identifying hammerstein model nonlinear systems," in *Proceedings of the 15th IEEE Conference on Decision and Control*, pp. 934–938, IEEE, Clearwater, FL, USA, December 1976.
- [16] E. W. Bai and M. Fu, "A blind approach to Hammerstein model identification," *IEEE Transactions on Signal Processing*, vol. 50, no. 7, pp. 1610–1619, 2002.
- [17] Z. Liao, Z. Zhu, S. Liang, C. Peng, and Y. Wang, "Subspace identification for fractional order Hammerstein systems based on instrumental variables," *International Journal of Control, Automation and Systems*, vol. 10, no. 5, pp. 947–953, 2012.
- [18] W. Greblicki, "Nonlinearity estimation in Hammerstein systems based on ordered observations," *IEEE Transactions on Signal Processing*, vol. 44, no. 5, pp. 1224–1233, 1996.
- [19] I. Goethals, K. Pelckmans, J. A. K. Suykens, and B. De Moor, "Identification of MIMO Hammerstein models using least squares support vector machines," *Automatica*, vol. 41, no. 7, pp. 1263–1272, 2005.
- [20] P. Van Overschee and B. De Moor, "N4SID: subspace algorithms for the identification of combined deterministic-stochastic systems," *Automatica*, vol. 30, no. 1, pp. 75–93, 1994.
- [21] W. E. Larimore, "Canonical variate analysis in identification, filtering, and adaptive control," in *Proceedings of the 29th IEEE Conference on Decision and Control*, pp. 596–604, IEEE, Honolulu, HI, USA, December 1990.
- [22] J. C. Gómez and E. Baeyens, "Subspace-based identification algorithms for Hammerstein and Wiener models," *European Journal of Control*, vol. 11, no. 2, pp. 127–136, 2005.
- [23] Z. Rayouf, C. Ghorbel, and N. B. Braiek, "A new Hammerstein model control strategy: feedback stabilization and stability analysis," *International Journal of Dynamics and Control*, vol. 7, no. 4, pp. 1453–1461, 2019.
- [24] W. M. Haddad and V. Chellaboina, "Nonlinear control of Hammerstein systems with passive nonlinear dynamics," *IEEE Transactions on Automatic Control*, vol. 46, no. 10, pp. 1630–1634, 2001.
- [25] T. Knohl, W. M. Xu, and H. Unbehauen, "Indirect adaptive dual control for Hammerstein systems using ann," *Control Engineering Practice*, vol. 11, no. 4, pp. 377–385, 2003.
- [26] H. Wang, J. Zhao, Z. Xu, and Z. Shao, "Linear model predictive control for hammerstein system with unknown nonlinearities," *IFAC Proceedings Volumes*, vol. 46, no. 13, pp. 302–306, 2013.
- [27] C. Ghorbel, Z. Rayouf, and N. Benhadj Braiek, "Robust stabilization and tracking control schemes for disturbed multi-input multi-output Hammerstein model in presence of approximate polynomial nonlinearities," *Proceedings of the Institution of Mechanical Engineers, Part I: Journal of Systems and Control Engineering*, vol. 101, 2020.
- [28] Z. Rayouf, C. Ghorbel, and N. B. Braiek, "Identification and nonlinear PID control of Hammerstein model using polynomial structures," *International Journal of Advanced Computer Science and Applications*, vol. 8, no. 4, pp. 488–493, 2017.
- [29] X. Hong and R. J. Mitchell, "Hammerstein model identification algorithm using Bezier-Bernstein approximation," *IET Control Theory & Applications*, vol. 1, no. 4, pp. 1149–1159, 2007.
- [30] X. Hong, R. J. Mitchell, and S. Chen, "Modelling and control of Hammerstein system using B-spline approximation and the inverse of De Boor algorithm," *International Journal of Systems Science*, vol. 43, no. 10, pp. 1976–1984, 2012.
- [31] S. Chen, X. Hong, J. Gao, and C. J. Harris, "Complex-valued B-spline neural networks for modeling and inverting Hammerstein systems," *IEEE Transactions on Neural Networks and Learning Systems*, vol. 25, no. 9, pp. 1673–1685, 2014.
- [32] X. Chang, "Robust non-fragile H_∞ filtering of fuzzy systems with linear fractional parametric uncertainties," *IEEE Transactions on Fuzzy Systems*, vol. 20, no. 6, pp. 1001–1011, 2012.
- [33] N. Vafamand, M. H. Asemiani, and A. Khayatian, "TS fuzzy robust L 1 control for nonlinear systems with persistent bounded disturbances," *Journal of the Franklin Institute*, vol. 354, no. 14, pp. 5854–5876, 2017.
- [34] H. Wang, S. Xie, B. Zhou, and W. Wang, "Non-fragile robust H_∞ filtering of Takagi-Sugeno fuzzy networked control

- systems with sensor failures,” *Sensors*, vol. 20, no. 1, pp. 1–16, 2020.
- [35] A. Tiga, N. B. Braiek, and C. Ghorbel, “Proportional PDC design-based robust stabilization and tracking control strategies for uncertain and disturbed T-S model,” *Complexity*, vol. 1, pp. 1–9, 2020.
- [36] Y. Zhang, G.-Y. Tang, and N.-P. Hu, “Non-fragile control for nonlinear networked control systems with long time-delay,” *Computers & Mathematics with Applications*, vol. 57, no. 10, pp. 1630–1637, 2009.
- [37] F. Xingjian, L. Xiaohe, H. Ming, and L. Yingchun, “Robust non-fragile control for non-linear singular discrete systems with time-delay,” in *Proceedings of the 10th World Congress on Intelligent Control and Automation*, pp. 1139–1143, IEEE, Beijing, China, July 2012.
- [38] J. W. Lee, H. H. Lee, J. K. Kim, and H. B. Park, “Robust and non-fragile fuzzy H_∞ controller design for discrete-time systems with parameter uncertainties and time delay,” in *Proceedings of the 2009 International Conference on Information and Automation*, pp. 722–727, IEEE, Zhuhai, China, June 2009.
- [39] N. Vafamand, M. M. Arefi, and A. Khayatian, “Nonlinear system identification based on Takagi-Sugeno fuzzy modeling and unscented Kalman filter,” *ISA Transactions*, vol. 74, pp. 134–143, 2018.
- [40] N. Vafamand, “Global non-quadratic Lyapunov-based stabilization of T-S fuzzy systems: a descriptor approach,” *Journal of Vibration and Control*, vol. 26, no. 19-20, pp. 1765–1778, 2020.
- [41] Y. Zhu, “Estimation of an N-L-N hammerstein-wiener model,” *IFAC Proceedings Volumes*, vol. 35, no. 1, pp. 247–252, 2002.
- [42] J. C. Gómez and E. Baeyens, “Subspace identification of multivariable Hammerstein and Wiener models,” *IFAC Proceedings Volumes*, vol. 35, no. 1, pp. 55–60, 2002.
- [43] D. Rotondo, F. Nejjari, and V. Puig, “Quasi-LPV modeling, identification and control of a twin rotor MIMO system,” *Control Engineering Practice*, vol. 21, no. 6, pp. 829–846, 2013.